Structural Changes Caused by Site-Directed Mutagenesis of Tyrosine-98 in *Desulfovibrio vulgaris* Flavodoxin Delineated by ^{1}H and ^{15}N NMR Spectroscopy: Implications for Redox Potential Modulation†

Brian J. Stockman,*,‡ Thomas E. Richardson,‡,§ and Richard P. Swenson‖

Upjohn Laboratories, The Upjohn Company, 301 Henrietta Street, Kalamazoo, Michigan 49007, and Department of Biochemistry, The Ohio State University, Columbus, Ohio 43210

Received June 24, 1994; Revised Manuscript Received October 16, 1994⊗

ABSTRACT: Flavodoxins mediate electron transfer at low redox potential between the prosthetic groups of other proteins. Interactions between the protein and the flavin mononucleotide cofactor shift both the oxidized/semiquinone and semiquinone/hydroquinone redox potentials significantly from their free-in-solution values. In order to investigate the possible role that the tyrosine at position 98 plays in this process, we have used heteronuclear three-dimensional NMR spectroscopy to determine the solution conformation of wild-type and four position-98 mutants, Y98W, Y98H, Y98A, and Y98R, of *Desulfovibrio vulgaris* flavodoxin. Assigned ^{1}H and ^{15}N resonances indicate that the secondary structure and topology of the proteins are identical. However, residues that undergo substantial mutation-induced changes in chemical shift are spread throughout the flavin cofactor binding site. Distance and dihedral angle constraints were used to generate solution structures for the wild-type and mutant proteins. Collectively, the mutant proteins have no gross conformational changes in the flavin binding site. The changes that do occur are minor and result from the different packing interactions required to accommodate the new side chain at position-98. The solvent accessibility and electrostatic nature of the flavin binding site in the mutant proteins are compared to those of the wild-type structure. The structural data support the hypothesis that the very low midpoint of the semiquinone/hydroquinone couple in the wild-type protein is modulated to a large extent by the energetically unfavorable formation of the flavin hydroquinone anion in the apolar environment of the flavin binding site.

Flavodoxins are FMN[1] -containing proteins that mediate electron transfer at low redox potential between the prosthetic groups of other proteins (Mayhew & Ludwig, 1975). The flavin cofactor has three oxidation states: oxidized, semiquinone (one-electron reduced), and hydroquinone (two-electron reduced). Protein−flavin mononucleotide interactions shift both the oxidized/semiquinone and semiquinone/hydroquinone redox potentials significantly from their free-in-solution values. In *Desulfovibrio vulgaris* flavodoxin the oxidized/semiquinone couple is −148 mV and the semiquinone/hydroquinone couple is −443 mV (Swenson & Krey, 1994), while those of free flavin are −238 and −172 mV, respectively (Simondson & Tollin, 1980). Understanding specific protein−cofactor interactions that underlie the altered redox potentials is paramount to understanding the electron-transfer processes that involve flavodoxins. Structure−function relationships determined for the flavodoxin system should be specifically applicable to other flavoproteins and generally applicable to other types of electron-transfer proteins.

Structures of flavodoxins from a variety of organisms have been elucidated by X-ray crystallographic methods, including *Clostridium beijerinckii* (Ludwig & Luschinsky, 1992), *D. vulgaris* (Watt et al., 1991), *Anacystis nidulans* (Smith et al., 1983), *Anabaena* 7120 (Rao et al., 1992), and *Chondrus crispus* (Fukuyama et al., 1990). In addition, NMR spectroscopy has been used to investigate the solution structures of flavodoxins from *Megasphaera elsdenii* (van Mierlo et al., 1990), *D. vulgaris* (Knauf et al., 1993; Stockman et al., 1993), *A.* 7120 (Stockman et al., 1990), and *A. nidulans* (Clubb et al., 1991). However, structural differences in the FMN binding site have proven difficult to correlate with the observed variations in redox potentials (Paulsen et al., 1990; Ludwig & Luschinsky, 1992). Several mechanisms have been hypothesized to explain the redox potential modulation, including distortion of the flavin ring system (Hall et al., 1987), steric hindrance to protonation of the flavin N^1 atom (Ludwig et al., 1990), repulsive interactions between the negatively-charged flavin phosphate group or side chains in the flavin binding site and the hydroquinone anion (Moonen et al., 1984), and formation of the hydroquinone anion in a relatively nonpolar environment (Ludwig et al., 1990). Evidence in support of the latter mechanism has been obtained by determining the redox properties of several position-98 mutants of *D. vulgaris* flavodoxin (Swenson &

† Supported by NIH Grant GM 36490 to R.P.S.

* To whom correspondence should be addressed.

‡ Upjohn Laboratories.

§ Present address: Department of Chemistry, University of South Carolina.

‖ The Ohio State University.

⊗ Abstract published in *Advance ACS Abstracts,* December 1, 1994.

[1] Abbreviations: FMN, flavin mononucleotide; HMQC, heteronuclear multiple-quantum correlation; HSQC, heteronuclear single-quantum correlation; NMR, nuclear magnetic resonance; NOESY, nuclear Overhauser enhancement spectroscopy; NOE, nuclear Overhauser enhancement; TOCSY, total correlation spectroscopy; Y98A, flavodoxin with alanine substituted for tyrosine at position 98; Y98H, flavodoxin with histidine substituted for tyrosine at position 98; Y98R, flavodoxin with arginine substituted for tyrosine at position 98; Y98W, flavodoxin with tryptophan substituted for tyrosine at position 98.

0006-2960/94/0433-15298$04.50/0

Krey, 1994). In that study, substantial increases in the midpoint potential of the semiquinone/hydroquinone couple were noted for the Y98A mutant in which the flavin isoalloxazine ring has greater solvent exposure and also for the Y98H and Y98R mutants in which favorable electrostatic interactions with the flavin hydroquinone anion are postulated. In order to provide structural information to complement the functional studies, we have used heteronuclear three-dimensional NMR spectroscopy to determine the solution conformation of wild-type *D. vulgaris* flavodoxin and four position-98 mutants, Y98W, Y98H, Y98A, and Y98R.

Previously, we have determined sequential ^1H and ^{15}N resonance assignments for the oxidized wild-type protein (Stockman et al., 1993). In the process, the solution secondary structure of the protein was elucidated, and several protein−FMN interactions were identified. Here we extend our investigation to include ^1H and ^{15}N resonance assignments for four single-site mutants of *D. vulgaris* flavodoxin, Y98W, Y98H, Y98R, and Y98A. Differences and similarities between the chemical shifts of the wild-type and mutant flavodoxins provide a qualitative picture of the structural consequences of the mutations. Differences were also observed in the patterns of protein−cofactor and protein−protein NOE's, as well as for several backbone ϕ angles. Details of the mutation-induced structural changes were obtained by using the collection of NMR constraints to calculate the solution conformation of each protein, especially with regard to the cofactor binding site. Since the redox potentials of all five species have been determined previously (Swenson & Krey, 1994), the structural data for the mutant proteins can be compared to those for the wild-type structure in the context of redox potential differences.

MATERIALS AND METHODS

Protein Enrichment and Sample Preparation. Recombinant *D vulgaris* (Hildenborough) flavodoxin was prepared as described previously (Krey et al., 1988). The protein used for NMR studies differs from the naturally-occurring protein in that the N-terminal methionine has been cleaved off and the proline at the next position has been replaced by an alanine. For comparisons with flavodoxins from other species, the numbering system in this paper begins with the N-terminal alanine as residue number two. The single-site mutant proteins Y98W, Y98H, Y98R, and Y98A were prepared as described previously (Swenson & Krey, 1994). Uniformly ^{15}N-enriched flavodoxins were prepared by using M9 minimal media in place of rich media. $^{15}NH_4Cl$ was supplied at a level of 1 g/L as the sole nitrogen source. Since the flavin cofactor is not supplied in the growth media and must be synthesized from small molecule precursors, the nitrogen atoms of the isoalloxazine ring were ^{15}N-enriched as well during this process. Samples for NMR experiments typically contained 2 mM flavodoxin in 100 mM phosphate buffer at pH 6.5. Trace amounts of PMSF and NaN_3 were added to prevent any protease digestion or bacterial growth in the sample. The pH, buffer concentrations, and temperature for the wild-type and mutant flavodoxins were identical in order to minimize the effect of these variables on ^1H and ^{15}N chemical shifts.

NMR Spectroscopy. All NMR spectra were recorded at 300 K on a Bruker AMX-600 spectrometer equipped with a multichannel interface. Proton chemical shifts were referenced to the ^1H_2O signal at 4.76 ppm. Nitrogen chemical shifts were referenced to external $^{15}NH_4Cl$ (2.9 M) in 1 M HCl at 24.93 ppm relative to liquid ammonia. Spectra were processed on a Silicon Graphics Personal Iris 4D35 workstation using the software package FELIX from Hare Research, Inc. Two-dimensional $^1H-^{15}N$ HSQC and $^1H-^{15}N$ HMQC-J and three-dimensional $^1H-^{15}N$ NOESY-HMQC, $^1H-^{15}N$ TOCSY-HMQC, and $^1H-^{15}N$ HMQC-NOESY-HMQC spectra were recorded and processed in an identical manner as was done for the wild-type protein (Stockman et al., 1993). A mixing time of 100 ms was used for each NOESY experiment. For each mutant, the complete battery of heteronuclear NMR experiments was recorded over a 10-day time period using the same sample.

Structure Calculations. Restrained energy minimization calculations were performed on a Silicon Graphics Iris Crimson server using the program Discover from Biosym Technologies, Inc. All calculations used the X-ray crystallographic structure (Watt et al., 1991) as the starting point. This was deemed appropriate since all NOE constraints obtained for the wild-type protein were consistent with this 2.0 Å resolution structure. For the mutant proteins, the residue at position 98 was replaced with the appropriate side chain. Because of the importance of water molecules on surface features, each protein was solvated with water prior to the calculations. This was accomplished by using the *soak* command with a layer thickness of 5.0. A total of 691, 696, 678, 677, and 690 NMR-derived constraints were used in the wild-type (122 distance, 482 NOE, 87 dihedral), Y98W (122 distance, 490 NOE, 84 dihedral), Y98H (122 distance, 470 NOE, 86 dihedral), Y98A (122 distance, 472 NOE, 83 dihedral), and Y98R (122 distance, 483 NOE, 85 dihedral) calculations, respectively. The interproton distance constraints were all interresidue. Although several hundred intraresidue NOE's were also assigned, they were not incorporated into the structure calculations since they provided little meaningful information. Assigned NOE's were classified as strong, medium, or weak. Corresponding upper bound constraints were 3.0, 4.0, and 5.0 Å. The lower bound constraints used in the calculations were the van der Waals contact radii. The NOE-derived distance constraints were supplemented with 116 distance constraints assigned to hydrogen bonds on the basis of slowly exchanging amide protons (Stockman et al., 1993). Constraints on ϕ angles were also incorporated into the calculations when they could be obtained from the $^1H-^{15}N$ HMQC-J spectra. ϕ values were constrained between $-170°$ and $-80°$ for $^3J_{HN\alpha}$ values >8 Hz and between $-90°$ and $-10°$ for $^3J_{HN\alpha}$ values <6 Hz. A listing of all constraints, highlighting the differences between the wild-type and mutant proteins, is provided in the supplementary material. In addition to the NMR-derived constraints, six hydrogen-bond constraints were imposed to anchor the phosphate group of the flavin cofactor into the binding site. This was necessary since there are no protons on the phosphate group from which to obtain protein−cofactor distance constraints. The distance limits for these constraints in each calculation were set to the corresponding distances in the X-ray structure since the chemical shifts of residues in this part of the FMN binding site are very similar to those of the wild-type protein, indicating that the phosphate binding site is conserved in the mutant proteins. For each protein, three rounds of restrained energy minimization were

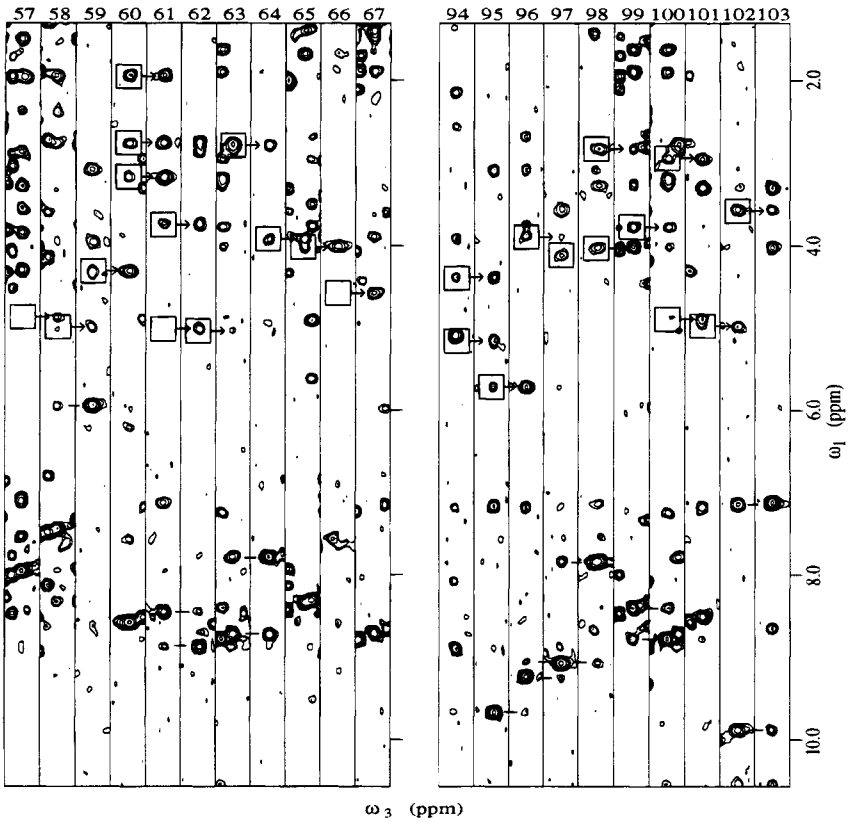

FIGURE 1: ω_1,ω_3 slices from the 3D $^1H-^{15}N$ NOESY-HMQC spectrum of the Y98W mutant, illustrating the sequential assignment of residues 57−67 and 94−103. Slices are taken at the ^{15}N frequency corresponding to the residue indicated at the top of each panel. Each slice represents 0.19 ppm in ω_3, with the center located at the frequency of the indicated $^1H^N$ resonance. Intraresidue $d_{N\alpha}$ and $d_{N\beta}$ correlations are boxed. Sequential $d_{N\alpha}(i,i-1)$ and $d_{N\beta}(i,i-1)$ correlations are indicated by arrows beginning at the boxed intraresidue correlation in the preceding slice. Horizontal lines identify sequential d_{NN} NOE's. Empty boxes correspond to intraresidue correlations, such as the cysteine-57 and serine-58 $d_{N\alpha}$ correlations, that are weak or completely missing at the level plotted. However, a correlation is seen at the corresponding position in the $^1H-^{15}N$ TOCSY-HMQC spectrum.

performed, each consisting of 2000 cycles of steepest descents and 10 000 cycles of conjugant gradients. Force constants used were 40 kcal/(mol·Å^2) for distance constraints and 40 kcal/(mol·rad^2) for torsion angle constraints.

RESULTS

Sequential assignments for the majority of main-chain ^1H and ^{15}N resonances for each of the single-site mutant flavodoxins were obtained by direct comparison of the wild-type and mutant $^1H-^{15}N$ HSQC spectra. Superimposition of the $^1H-^{15}N$ correlations for close to 80% of the main-chain amide groups in the wild-type and each mutant protein made this possible. The remaining 20% of the resonances were shifted in the mutant flavodoxins compared to the wild-type protein, and their assignments were thus not straightforward. Assignments for these residues were made using a combination of $^1H-^{15}N$ NOESY-HMQC, $^1H-^{15}N$ TOCSY-HMQC, and $^1H-^{15}N$ HMQC-NOESY-HMQC spectra, analogous to what was done for the wild-type protein (Stockman et al., 1993). For completeness, the assignments for the 80% of the residues in each mutant that had chemical shifts nearly identical to wild-type were verified by direct comparison of the three-dimensional $^1H-^{15}N$ NOESY-HMQC and $^1H-^{15}N$ TOCSY-HMQC data sets obtained for the mutant and wild-type proteins.

Regions in the primary sequence with the largest chemical shift changes were residues 57−67 and 94−103 in Y98W and Y98H, and residues 94−103 and 125−129 in Y98R and Y98A. Sequential assignments for these residue stretches in each mutant will be detailed briefly. The data strips shown are representative of the quality of data obtained for each mutant. Each panel represents a small ω_1,ω_3 slice of the $^1H-^{15}N$ NOESY-HMQC spectrum corresponding to the $^1H^N$ group of the residue indicated. Intraresidue NOE's, distinguished from interresidue NOE's by comparison to the corresponding region of the $^1H-^{15}N$ TOCSY-HMQC spectrum, are boxed. Arrows drawn indicate sequential $d_{N\alpha}(i,i-1)$ and $d_{N\beta}(i,i-1)$ NOE's used to make the assignments. Horizontal lines identify sequential d_{NN} NOE's.

Assignment of residues 57−67 and 94−103 of the Y98W and Y98H mutants are illustrated in Figures 1 and 2, respectively. For Y98W, sequential $d_{N\alpha}(i,i-1)$ NOE's were observed for all residues except serine-64 and tyrosine-98. Assignments for these two residues were based on the observation of strong $d_{NN}(i,i-1)$ NOE's and $d_{N\alpha}(i,i-1)$ NOE's for the subsequent residue. For Y98H, sequential $d_{N\alpha}(i,i-1)$ NOE's were observed for all residues except aspartic acid-63 and serine-64. Serine-64 was assigned based on $d_{N\alpha}(i,i-1)$ and $d_{N\beta}(i,i-1)$ NOE's for isoleucine-65. Aspartic acid-63 was assigned based on a d_{NN} NOE to serine-64. No sequential connectivities between aspartic acid-62 and aspartic acid-63 were identified.

Assignment of residues 94−103 and 125−129 of the Y98A and Y98R mutants is illustrated in Figures 3 and 4, respectively. For Y98A, sequential $d_{N\alpha}(i,i-1)$ NOE's were observed for all residues. For Y98R, sequential $d_{N\alpha}(i,i-1)$ NOE's were observed for all residues except phenylalanine-101. Assignment of phenylalanine-101 was based on the

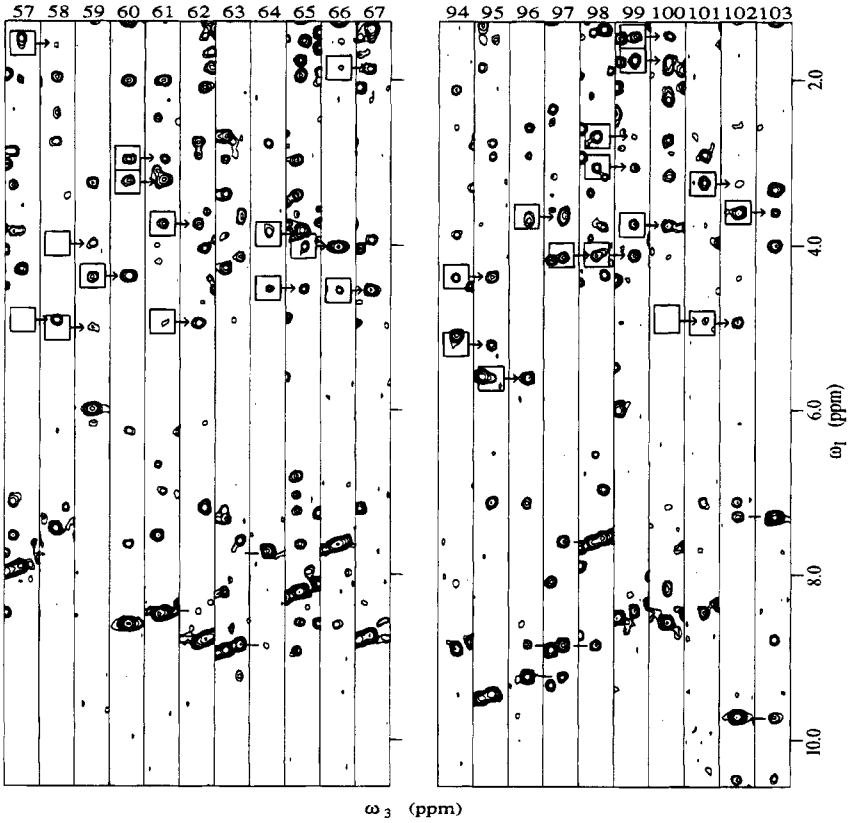

FIGURE 2: ω_1,ω_3 slices from the 3D $^1H-^{15}N$ NOESY-HMQC spectrum of the Y98H mutant, illustrating the sequential assignment of residues 57−67 and 94−103. Slices are annotated analogous to those in Figure 1.

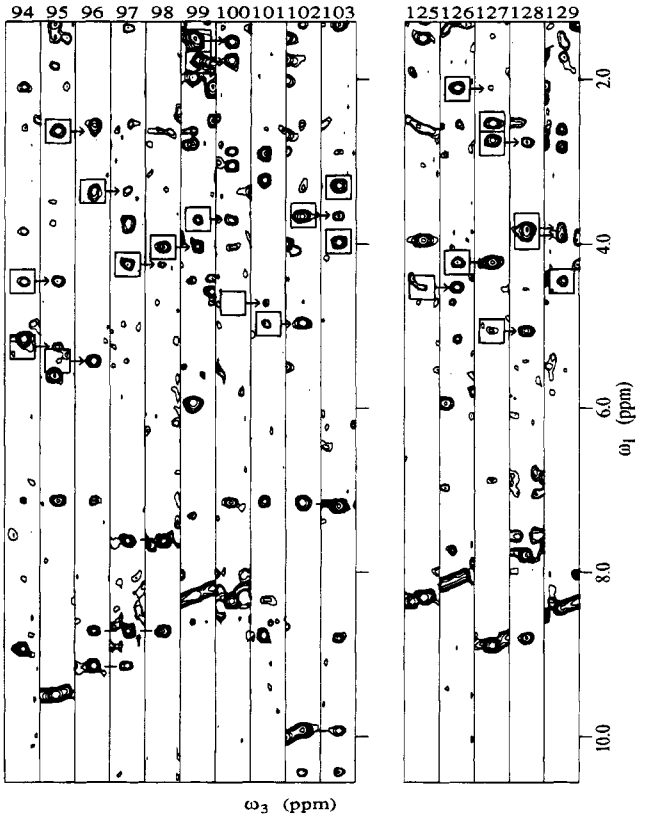

FIGURE 3: ω_1,ω_3 slices from the 3D $^1H-^{15}N$ NOESY-HMQC spectrum of the Y98A mutant, illustrating the sequential assignment of residues 94−103 and 125−129. Slices are annotated analogous to those in Figure 1.

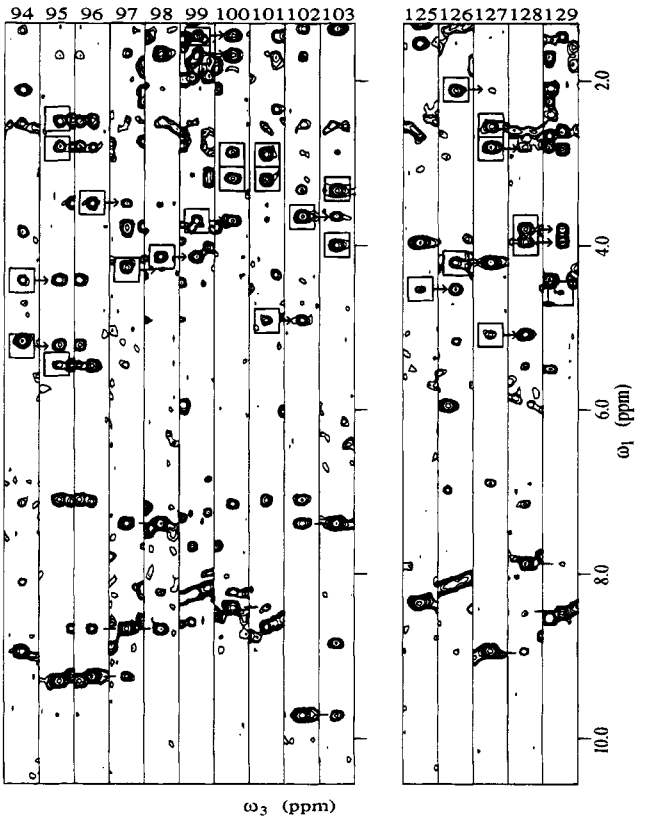

FIGURE 4: ω_1,ω_3 slices from the 3D $^1H-^{15}N$ NOESY-HMQC spectrum of the Y98R mutant, illustrating the sequential assignment of residues 94−103 and 125−129. Slices are annotated analogous to those in Figure 1.

observation of a strong $d_{NN}(i,i-1)$ NOE to tyrosine-100 and a $d_{N\alpha}(i,i-1)$ NOE for cysteine-102.

For each mutant, side-chain assignments were made for many of the residues based on the $^1H-^{15}N$ TOCSY-HMQC

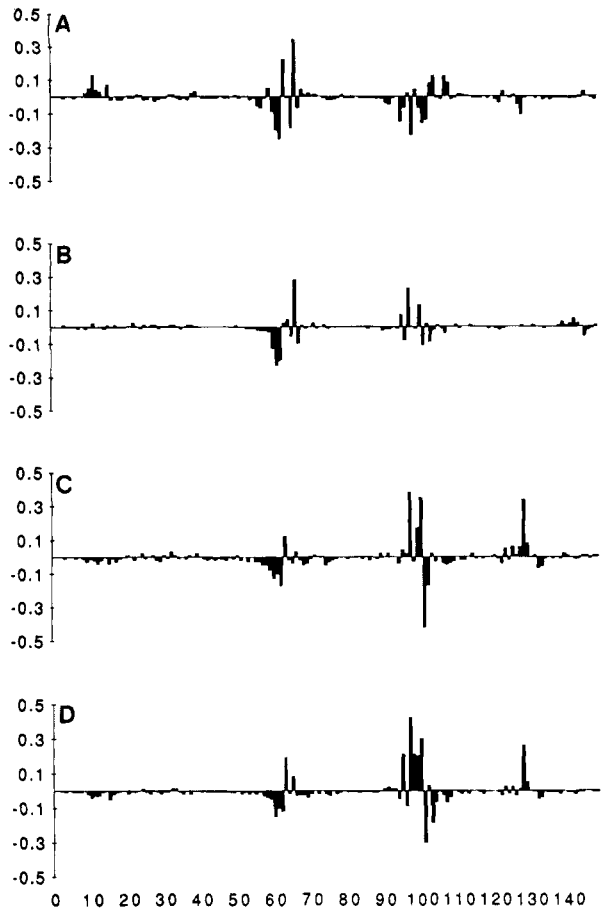

FIGURE 5: Comparison of the differences in chemical shift ($\Delta\delta$) between the wild-type and mutant flavodoxins observed for the $^1H^N$ resonance plotted as a function of residue number. (A) Y98W, (B) Y98H, (C) Y98A, and (D) Y98R.

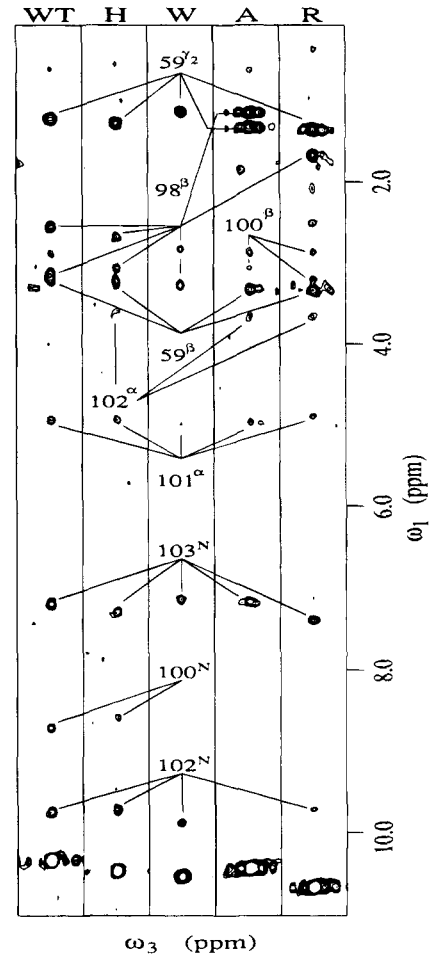

FIGURE 6: ω_1,ω_3 slices from the 3D $^1H-^{15}N$ NOESY-HMQC spectra of the wild-type and four mutant flavodoxins, illustrating the pattern of NOE's observed that involve the $^1H^{N3}$ proton of the flavin cofactor. Each slice is taken at the ^{15}N frequency of the flavin $^{15}N^3$ nitrogen, with the center located at the frequency of the flavin $^1H^{N3}$ proton resonance. Assigned NOE's in ω_1 are labeled according to residue number and atom type.

spectrum. Overall, the chemical shifts were commensurate with the amino acid type and were quite similar to those determined for the wild-type protein. However, the chemical shifts for several protons of the various position-98 side chains are ring-current shifted to high field because of their proximity to the flavin isoalloxazine ring. As discussed below, analysis of these shifts orients the position-98 side chain with respect to the flavin ring. A summary of all assigned ^1H and ^{15}N chemical shifts for each mutant is provided as supplementary material.

Inspection of Figure 5 delineates regions of the primary sequence that have nearly identical $^1H^N$ chemical shifts in the wild-type and mutant flavodoxins, as well as regions that have differences in chemical shifts. Similar plots were obtained for the $^{15}N^{\alpha}$ chemical shifts (not shown). Around 80% of the residues have nearly identical chemical shifts in each of the five species, indicating that the secondary structure and topology of the proteins are identical. Thus the mutations have not drastically altered the conformation of the protein. As expected, residues in each mutant protein that are near position 98 in the linear amino acid sequence (90's loop) experience changes in their chemical shifts because of changes in their local environment. However, residues with altered chemical shifts are not limited to those in the 90's loop. Instead, residues that undergo substantial mutation-induced changes in chemical shift are spread throughout the flavin cofactor binding site. For all four mutants, chemical shift changes are observed in the 60's loop. In addition, chemical shift changes in the 120's region were observed for the Y98A and Y98R mutants, and very small chemical shift changes in the phosphate binding region were observed for the Y98W mutant. The locations of the affected residues with respect to the flavin cofactor are shown in Figure 8A. Chemical shift changes arise from both structural changes and differences in the intrinsic nature of the various side chains at position 98. Contributions from the latter are greatest for the Y98A and Y98R mutants since they result in the removal of an aromatic side chain. This may be reflected in the larger $\Delta\delta$ values observed for residues in the 90's loop (Figure 5).

During the assignment process, NOE's between the $^1H^{N3}$ proton of the flavin cofactor and protons of residues located nearby in the folded structure were observed in the $^1H-^{15}N$ NOESY-HMQC spectra. The various NOE's observed and their relative intensities for each mutant protein compared to the wild-type protein provide structural insights into mutation-induced changes in this side of the FMN binding site. A comparison of observed FMN $^1H^{N3}$ NOE's is shown in Figure 6. The panels are analogous to those in Figures 1−4. The FMN $^1H^{N3}$ proton of the wild-type and those of each mutant flavodoxin have an NOE to the backbone $^1H^N$ proton of glycine-103, the $^1H^{\alpha}$ proton of phenylalanine-101, and the $^1H^{\beta}$ and $^1H^{\gamma}$ protons of threonine-59. However, the NOE intensities show some variations between the different

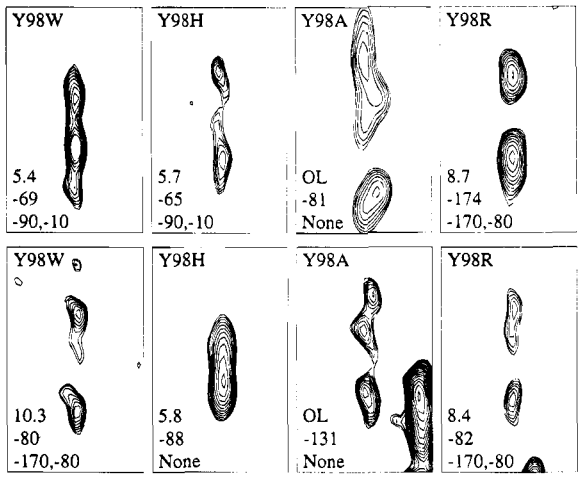

FIGURE 7: Regions of the $^1H-^{15}N$ HMQC-J spectra corresponding to the aspartic acid-62 (top row) and aspartic acid-63 (bottom row) correlations in the four mutant flavodoxins. Three parameters are given in the bottom left corner of each panel: (top) value in Hz measured for the $^3J_{NH\alpha}$ coupling constant, (middle) value of the ϕ angle in the final calculated structure, and (bottom) ϕ angle range used in the structure calculation. "OL" indicates that resonance overlap precluded measurement of the coupling constant. "None" indicates that no range for the ϕ angle was used in the structure calculation.

protein species. More striking, however, is the observation of NOE's to the backbone $^1H^N$ proton of tyrosine-100 for the wild-type and Y98H flavodoxins, but not for Y98W, Y98A, or Y98R, as well as the observation of NOE's to the backbone $^1H^N$ proton of cysteine-102 for each flavodoxin species except Y98A. NOE's were also observed to the $^1H^\alpha$ proton of cysteine-102 for Y98H, Y98A, and Y98R, but not for the wild-type or Y98W proteins. Structural changes caused by mutation of the residue at position 98 are manifested in the different NOE patterns observed. Several differences in the relative intensities of protein−protein NOE's for residues in the flavin binding site were also observed (listed in the supplementary material), resulting in further quantitation of mutation-induced structure alterations.

Main-chain ϕ angles were monitored in the mutant proteins. Analysis of the HMQC-J spectra recorded for each mutant species indicated that the great majority of $^3J_{NH\alpha}$ coupling constants, related to the main-chain ϕ angle, were consistently similar between the mutant species and the wild-type protein. Most values for a given residue were within 1 Hz of each other for all five species, resulting in structural constraints on the ϕ angle being in the same region of conformational space. However, several residues in the flavin binding site had significantly different $^3J_{NH\alpha}$ values that resulted in structural constraints on the ϕ angle being in a different region of conformational space compared to the wild-type protein. The $^3J_{NH\alpha}$ value for aspartic acid-62 in the wild-type protein was previously found to be 8.5 Hz. As shown in the top row of Figure 7, a similar value was found for the Y98R mutant, but smaller values were observed for the Y98W and Y98H mutants. The value for the Y98A mutant could not be measured because of resonance overlap. Thus the ϕ angel restraint used for the Y98W and Y98H mutants was $-90°$ to $-10°$, in contrast to $-170°$ to $-80°$ used in the Y98R and wild-type calculations. Likewise, the aspartic acid-63 $^3J_{NH\alpha}$ value in the wild-type protein was found to be 3.5 Hz. As shown in the bottom row of panels in Figure 7, a similar value was found for the Y98H mutant, while the values were significantly larger in the Y98W and Y98R mutants. Again, the value for this coupling constant could not be determined for the Y98A mutant because of resonance overlap. The ϕ angle restraint range used for the Y98W and Y98R calculations was $-170°$ to $-80°$, while that used for the Y98H and wild-type calculations was $-90°$ to $-10°$. The only other $^3J_{NH\alpha}$ difference observed that was large enough to cause a change in the ϕ angle restraint range compared to the wild-type protein was for glutamic acid-66 in the Y98H mutant. The value was 8.6 Hz as compared to 5.0 Hz in the wild-type protein.

Differences in chemical shifts, NOE intensities, and coupling constants define the structural consequences of the replacement of the tyrosine at position 98 with different side chains. The latter two criteria were incorporated into restrained energy minimization calculations to obtain structures consistent with these restraints. The resulting structures of the flavin binding sites in the wild-type and mutant proteins are shown in Figure 8. Only the residues with the largest chemical shift changes in the mutant proteins, comprising the cofactor binding site, are shown. No distance violations greater than 0.1 Å nor any dihedral angle violations greater than 10° were present in any of the final calculated structures.

The X-ray crystallographic structure of the wild-type flavodoxin is completely consistent with the NMR constraints. Nonetheless, the solution structure was calculated in an analogous manner as was done for the mutant flavodoxins in order to provide a comparison to the solution structures calculated for the mutant flavodoxins. Any systematic differences introduced into the restrained-energy-minimized structures during the calculations, such as might be created by the solvation sphere, should be consistent for the wild-type and mutant proteins. The calculated wild-type structure provides a more meaningful basis for comparison of the mutant proteins than does the X-ray crystallographic structure. The flavin binding site of the wild-type flavodoxin is shown in Figure 8B. The largest difference between this structure and the X-ray crystallographic structure is that the tyrosine-98 aromatic ring and the FMN group are moved slightly less than half of an aromatic ring width closer to the surface of the protein. Concomitantly, residues 94−96 and 127−128, which interact with the inner edge of the cofactor, move in the same direction to maintain the same position relative to the cofactor. The tyrosine-98 aromatic ring and the flavin isoalloxazine ring systems maintain their coplanar orientation, but since the tryptophan-60 side chain remains in nearly the same position, it is located further from the flavin isoalloxazine ring in the calculated solution structure. The solvent accessibility of the flavin isoalloxazine ring is slightly different. In the X-ray crystallographic structure, only the outer edge of the xylene ring is solvent accessible. By contrast, in the NMR structure the area around N^3 and C^4 is solvent accessible, in addition to the outer edge of the xylene ring. This may be related to the observation of a bound water molecule (Wat155) in the X-ray structure, which forms hydrogen bonds to the backbone carbonyl oxygen of aspartic acid-62, the backbone amide nitrogen of tyrosine-100, and the FMN C^4 carbonyl oxygen (Watt et al., 1991). Solvent accessibility of the N^3-C^4 region is in agreement with fast exchange of the $^1H^{N3}$ proton with solvent reported previously (Stockman et al., 1993). The RMSD between the solution and X-ray crystallographic

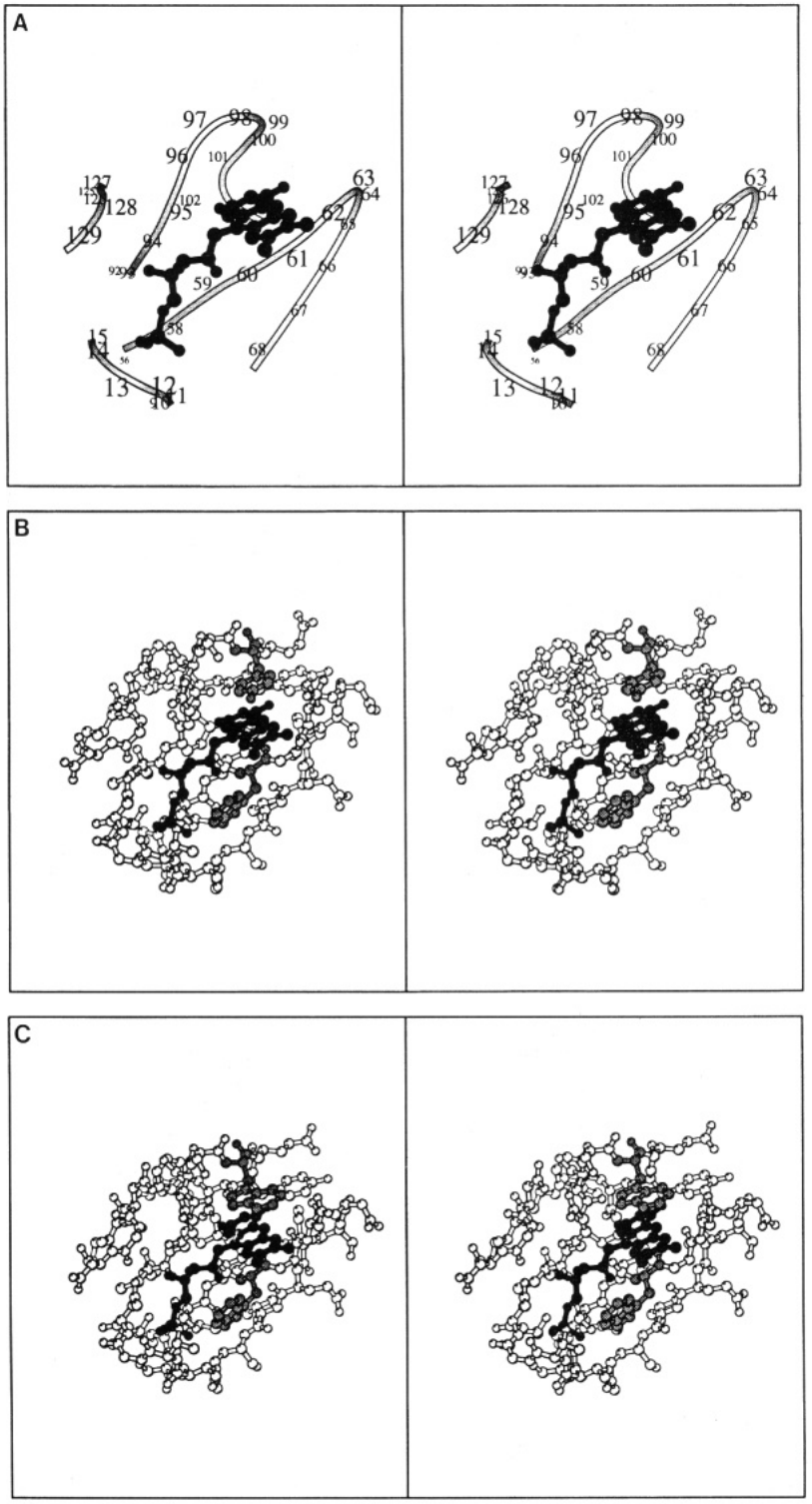

structures for the backbone atoms of the 38 residues shown in Figure 8B is 1.23 Å. For the remaining 109 residues of the two structures, the RMSD for the backbone atoms is 0.84 Å. The underlying reason for the small adjustment observed in the solution structure is not obvious. The same minor adjustment is seen in the solution structures calculated for each mutant as well and thus is not critical for understanding mutation-induced conformational changes that may be involved in redox potential modulation.

The restrained-energy-minimized solution structure of the Y98W mutant is shown in Figure 8C. The tryptophan side chain maintains a similar coplanar stacking interaction with the flavin isoalloxazine ring as is observed for the corresponding tyrosine side chain in the wild-type protein. The indole ring of the tryptophan side chain is positioned over the flavin ring system, similar to what has been seen in the X-ray crystallographic structure of the Y98W mutant (Reynolds et al., 1992; Watt et al., 1992). Both orientations of the tryptophan side chain (one as shown and one rotated 180° about the C^{β}-C^{γ} bond) were used as the starting conformation in separate restrained energy minimization calculations. The orientation shown in Figure 8C resulted in a lower final energy than the energy-minimized structure having the opposite orientation of this side chain. In addition, the

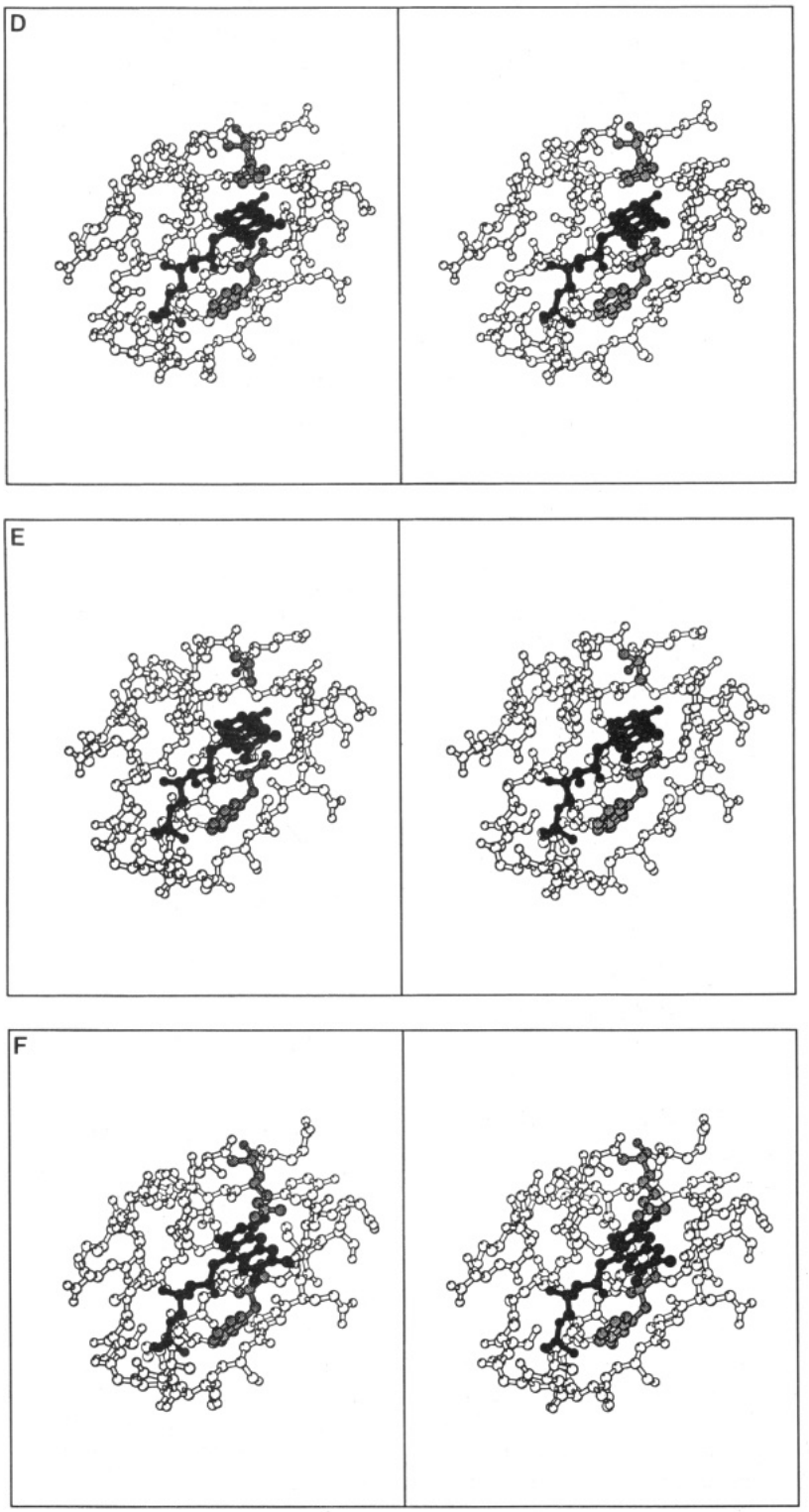

FIGURE 8: (A) Schematic of the FMN binding site. (B−F) Regions of the solution structures of the (B) wild-type, (C) Y98W, (D) Y98H, (E) Y98A, and (F) Y98R flavodoxins. Only residues in the flavin binding site are shown, including the following residues: 9−15, 56−68, 92−103, and 125−130, and the FMN group. The orientations are identical to (A). Tryptophan-60 and residue 98 are shown in light grey, while the FMN group is shown in dark grey. Only heavy atoms are shown. The figures were drawn using the program Molscript (Kraulis, 1991).

chemical shifts of the $^1H^{\zeta 2}$ (6.01 ppm) and $^1H^{\eta 2}$ (6.94 ppm) protons are shifted to high field by the flavin isoalloxazine ring, indicating that it is this edge of the tryptophan ring that is situated over the flavin ring. The coplanar configuration and extensive van der Waal contacts between the tryptophan side chain and the flavin isoalloxazine ring are consistent with the apparent strong electronic coupling of the indole and the flavin as evidenced by the unusual visible absorption spectrum for this mutant (Swenson & Krey, 1994). A pronounced absorbance band in the 500−700 nm region consistent with a charge transfer complex between the two is noted. The environment of the flavin cofactor is nearly identical to that calculated for the wild-type protein in terms of solvent accessibility and hydrophobicity. The RMSD

between the Y98W and wild-type solution structures for the backbone atoms of the 38 flavin binding site residues is 0.71 Å.

The restrained-energy-minimized solution structure of the Y98H mutant is shown in Figure 8D. As with the Y98W mutant, the histidine aromatic ring is positioned in a similar stacking interaction with the flavin isoalloxazine ring as is observed in the wild-type protein. The positive charge of the histidine side chain ($N^{\epsilon 2}$) is 2.9 Å away from the negatively charged aspartic acid-62 side chain ($O^{\delta 2}$). The positive charge introduced by the histidine side chain did not result in any major conformational rearrangement of the flavin binding site. This observation may result from the fact that residue 98 is near the surface of the protein, not buried in a hydrophobic environment. The introduction of a positive charge near the flavin cofactor, however, was found to have a large effect on the redox potentials, as discussed below. The solvent accessibility of the isoalloxazine ring is very similar to that in the wild-type solution structure. The RMSD between the Y98H and wild-type solution structures for the backbone atoms of the 38 flavin binding site residues is 0.55 Å.

The restrained-energy-minimized solution structure of the Y98A mutant is shown in Figure 8E. The side-chain methyl group is positioned very close to where the C^{β} of the tyrosine residue in the wild-type protein is positioned. The similarity in location of the C^{β} in Y98A, as well as in the other three mutants, as compared to the wild-type protein, is further evidenced by the $^1H^{\beta}$ $\Delta\delta$ values, which in all five proteins are slightly negative. The substitution of the smaller side chain has the effect of increasing the degree of solvent exposure of the flavin isoalloxazine ring since no rearrangements occur to replace the ring stacking interaction that exists in the wild-type protein. Half of the isoalloxazine ring system is solvent accessible, including all of the xylene ring and part of the pyrazine ring. Greater solvent accessibility is consistent with a higher level of fluorescence of the Y98A mutant compared to the wild-type and other mutant proteins (Swenson & Krey, 1994). The overall effect of the Y98A mutation then is to decrease the hydrophobic character of the flavin binding site. The RMSD between the Y98A and wild-type solution structures for the backbone atoms of the 38 flavin binding site residues is 0.67 Å.

The restrained-energy-minimized solution structure of the Y98R mutant is shown in Figure 8F. The side chain adopts an extended conformation, with the methylene groups above the bottom edge of the isoalloxazine ring system and the positively-charged guanidino group extending toward the xylene ring. This is further supported by the $^1H^{\gamma}$ (0.38 and 1.09 ppm) and $^1H^{\delta}$ (2.10 2.46 ppm) chemical shifts, which are shifted to high field by 0.8−1.3 ppm by their proximity to the flavin ring system. The flavin ring system is thus shielded from solvent as in the wild-type and all but the Y98A mutant proteins. The positive charge introduced by the Y98R mutant is located in a different position relative to the positive charge introduced by the Y98H mutant, but is still close enough to the cofactor to be involved in redox potential manipulation. The positive charge of the arginine side chain (C^{ζ}) is 3.9 Å away from the negatively-charged aspartic acid-62 side chain ($O^{\delta 2}$). The RMSD between the Y98R and wild-type solution structures for the backbone atoms of the 38 flavin binding site residues is 0.45 Å.

The calculated aspartic acid-62 ϕ angles satisfy the input restraint ranges. For the wild-type and Y98R mutants, the final ϕ angle is close to −170°. It should be noted that the aspartic acid-62 ϕ angle is +70° in the X-ray crystallographic structure. The observed $^3J_{NH\alpha}$ value of 8.5 Hz is consistent with both ϕ angles (Wüthrich, 1986). The difference between the X-ray and energy-minimized structure may be related to the interactions of this surface group with its surroundings. For the Y98W and Y98H mutants, the ϕ angle values are −69° and −65°, respectively. The change in conformational space observed for this angle in these two mutants is consistent with what has been observed by X-ray crystallographic methods (Reynolds et al., 1992; Watt et al., 1992). The Y98A ϕ, not restrained in the calculations, is −81°. In contrast, the calculated aspartic acid-63 ϕ angles ranged from −73° to −88° for those angles given restraint ranges. This result is obtained even though two of the restraint ranges were −170° to −80° (Y98W, Y98R) and two were −90° to −10° (Y98H and wild-type). It appears that, for aspartic acid-63, the preferred ϕ angle for the mutants is similar to the wild-type value of −83°. This contrasts with the X-ray results for Y98H and Y98W, which indicate that this angle is −125° and −145°, respectively (Reynolds et al., 1992; Watt et al., 1992). For Y98A, for which no restraint range was used, the ϕ angle was found to be −131°. The glutamic acid-66 ϕ angles calculated for the wild-type protein and Y98A mutant are −98°, somewhat outside the restraint range of −90° to −10°. The ϕ angles calculated for Y98W and Y98R, both unrestrained, as well as for Y98H, restrained to −170° to −80°, are around −130°. The value for the wild-type X-ray structure is −124°.

Collectively, the mutant proteins have no gross conformational changes in the flavin binding site. The changes that do occur are minor and result from the different packing interactions required to accommodate the new side chain at position 98. One noteworthy observation is that the distance between the flavin N^1 and the N^{α} of aspartic acid-95 ranges only from 2.94 to 3.01 Å in the five calculated structures. The variations in the 60's loop ϕ angles observed probably result from the fact that these residues are all on the surface of the protein and thus possess some degree of flexibility. Weaker NOE's involving the aspartic acid-62 and aspartic acid-63 $^1H^N$ protons are also indicative of flexibility in the 60's loop. It is interesting that the oxidized/semiquinone potentials are not very sensitive to the backbone perturbations in the 60's loop that are induced in the oxidized protein by the position-98 mutations (Swenson & Krey, 1994). This may imply that differential interactions of the 60's loop backbone with the flavin ring may not play as important a role in controlling the oxidized/semiquinone potentials in the *D. vulgaris* flavodoxin or that other compensatory interactions are introduced by these mutations. Further examination of this issue is required.

DISCUSSION

Values for the oxidation−reduction midpoint potentials for the wild-type and mutant flavodoxins have been determined previously (Swenson & Krey, 1994). The midpoint values for the oxidized/semiquinone couple range from −150 mV in the wild-type and Y98W proteins to around −180 mV in the Y98H, Y98A, and Y98R proteins. A much more drastic change is seen in the midpoints of the semiquinone/hydroquinone couple, where the values range from −450

mV in wild-type and Y98W proteins to −300 mV in the Y98A protein to −265 mV in the Y98H and Y98R proteins. The protein modulates this midpoint in such a manner that the values for the semiquinone/hydroquinone couple in the wild-type and mutant flavodoxins are all more negative than that for the flavin free in solution, which has a value of −172 mV for this couple (Simondson & Tollin, 1980).

The structural results presented here support the hypothesis that the very low midpoint of the semiquinone/hydroquinone couple in the wild-type protein is modulated to a large extent by the energetically unfavorable formation of the flavin hydroquinone anion in the apolar environment of the flavin binding site (Swenson & Krey, 1994). The similarity in the midpoint potentials of this couple for the wild-type and Y98W mutant results because the tyrosine and tryptophan side chains shroud the flavin ring with a large hydrophobic residue and are involved in similar ring stacking interactions with the isoalloxazine ring. By contrast, the removal of the bulky aromatic side chain in the Y98A mutant exposes more of the flavin ring system to solvent, reducing the hydrophobic character of the binding site. Formation of the hydroquinone anion is more favorable, resulting in an increase of the midpoint couple by about 150 mV. The Y98H and Y98R mutations further reduce the hydrophobic character of the cofactor binding site by introducing a positive charge in close proximity to the isoalloxazine ring. The imidazole ring of Y98H is coplanar with the flavin ring, situated over the pyrimidine and pyrazine rings, a configuration which should promote strong favorable electrostatic interactions between this side chain and the flavin hydroquinone anion. Interestingly, rather than extending out into solvent, the arginine side chain of the Y98R mutant is observed to extend along the isoalloxazine ring. This configuration places the positively charged guanidino group closer to the xylene ring of the flavin than is observed for the positively charged histidine ring in the Y98H mutant. Similar midpoint potentials for the semiquinone/hydroquinone couple are observed for these two mutants, however. Even if the histidine or arginine side chains were in their neutral form, which is not likely at pH 6.5 used for the NMR experiments, the hydrophobicity of the cofactor binding site would still be less than in the wild-type protein because of the intrinsic nature of these side chains. In fact, the midpoint potential for the Y98H mutant with the imidazole in its neutral form was estimated to be approximately 100 mV more positive than that of the wild-type (Swenson & Krey, 1994). When protonated, however, the histidine and arginine side chains favor the formation of the hydroquinone anion directly by providing a counterion in close proximity, and indirectly by offsetting the effects of the negatively-charged FMN phosphate group and other negatively-charged side chains in the flavin binding site. The overall effect is to make the midpoint couple more positive by almost 200 mV. The close contacts between the flavin and the side chain of the histidine in the Y98H mutant are also consistent with the predicted shift in the redox-linked ionization constant of this residue (Swenson & Krey, 1994).

Protonation of the hydroquinone anion has been found to occur only at very low pH, with the pK_a of the N^1 nitrogen shifted to less than 4.0 as compared to a value of 6.7 for the hydroquinone in solution. It has been proposed that suppression of protonation at N^1 is accomplished by close proximity of the polypeptide backbone to the N^1 position atom, leaving no room for protonation (Ludwig et al., 1990). In order for protonation to occur, rearrangement of the polypeptide backbone would have to occur. Instead of this unfavorable rearrangement, the hydroquinone anion is forced to exist in an unfavorable environment. Since in the structures determined here for the wild-type and mutant proteins the distance from the N^{α} nitrogen of aspartic acid-95 to the flavin N^1 atom remains close to 3.0 Å, the contribution of N^1 protonation steric hindrance to redox potential manipulation is similar for each mutant. The ultraviolet/visible absorbance spectrum of the hydroquinone is consistent with the presence of the flavin hydroquinone anion in each of these mutants (Swenson & Krey, 1994).

Propagation of conformational changes induced by mutations at position 98 to the adjacent 60's loop in the flavin binding site is not totally unexpected. Preliminary molecular modeling studies of several flavodoxins from the *Desulfovibrio* family suggest that sequence differences noted in the 90's loop can affect the conformation of residues in the 60's loop (Helms et al., 1990; Helms & Swenson, 1991; Helms and Swenson, unpublished results). The presence of a methionine residue at position 62 in the *Desulfovibrio desulfuricans* (Essex 6) flavodoxin, a position generally occupied by an acidic residue in this family, seems to influence the conformation of tyrosine-98 and the adjacent region (Helms & Swenson, 1992). Mutation of this methionine to an acidic residue substantially affects the midpoint potentials of the cofactor (Helms and Swenson, manuscript in preparation). A comparison of the *Desulfovibrio gigas* ATCC29494 flavodoxin, which has a histidine residue at position 100, with the *D. vulgaris* protein having a tyrosine at this position indicated small alterations in the conformation of the 60's loop. These changes may be the consequence of electrostatic interactions between the imidazole side chain and aspartate-62 and glutamate-64. The β-methyl group of the side chain of threonine-99 in the *D. gigas* flavodoxin may also account for some of the observed differences. Formation of specific side chain-to-side chain interactions across these two loops forming a large portion of the flavin binding site may thus be responsible for the alterations observed in the 60's loop for the mutants presented here. The contributions of these amino acid differences between the *D. gigas* and *D. vulgaris* proteins to the observed differences in the oxidation−reduction properties of these two proteins and the structure of the flavin binding site are currently being investigated through various mutagenesis studies (Helms, 1992 and unpublished results). It is likely that the results presented here, together with structural analyses of other flavodoxins within the *Desulfovibrio* family and various mutants with altered flavin binding sites, will lead to a clearer understanding as to how these proteins can so dramatically alter the oxidation−reduction and other physical and chemical properties of the versatile flavin coenzyme.

CONCLUSIONS

The structural consequences of incorporating various side chains at position 98 in *D. vulgaris* flavodoxin have been investigated. Mutation-induced changes were found to be localized to and dispersed throughout the flavin cofactor binding site. None of the mutations caused gross conformational changes, only minor ones resulting from the different packing interactions required to accommodate the new side chain at position-98. The Y98W mutation resulted

in the smallest changes in the flavin environment, while the Y98A mutation increased the solvent accessibility of the cofactor and the Y98H and Y98R mutations altered the cofactor's electrostatic environment. The structural data support the hypothesis that the very low midpoint of the semiquinone/hydroquinone couple in the wild-type protein is modulated to a large extent by the energetically unfavorable formation of the flavin hydroquinone anion in the apolar environment of the flavin binding site.

ACKNOWLEDGMENT

Discussions with Drs. T. Scahill, K. Watenpaugh, and W. Watt are appreciated.

SUPPLEMENTARY MATERIAL AVAILABLE

Two tables containing a list of structure constraints for the wild-type and four mutant proteins and assigned ^{1}H and ^{15}N chemical shifts for the mutant proteins (30 pages). Ordering information is given on any current masthead page.

REFERENCES

Clubb, R. T., Thanabal, V., Osborne, C., & Wagner, G. (1991) *Biochemistry 30*, 7718−7730.

Fukuyama, K., Wakabayashi, S., Matsubara, H., & Rogers, L. J. (1990) *J. Biol. Chem. 265*, 15804−15812.

Hall, L. H., Bowers, M. L., & Durfor, C. N. (1987) *Biochemistry 26*, 7401−7409.

Helms, L. R. (1992) Ph.D. Thesis, The Ohio State University.

Helms, L. R., & Swenson, R. P. (1991) *Biochim. Biophys. Acta 1089*, 417−419.

Helms, L. R., & Swenson, R. P. (1992) *Biochim. Biophys. Acta 1131*, 325−328.

Helms, L. R., Krey, G. D., & Swenson, R. P. (1990) *Biochem. Biophys. Res. Commun. 168*, 809−817.

Knauf, M. A., Löhr, F., Curley, G. P., O'Farrell, P., Mayhew, S. G., Müller, F., & Rüterjans, H. (1993) *Eur. J. Biochem. 213*, 167−184.

Kraulis, P. (1991) *J. Appl. Crystallogr. 24*, 946−950.

Krey, G. D., Vanin, E. F., & Swenson, R. P. (1988) *J. Biol. Chem. 263*, 15436−15443.

Ludwig, M. L., & Luschinsky, C. L. (1992) in *Chemistry and Biochemistry of Flavoenzymes* (Müller, F., Ed.) Vol. 3, pp 427−466, CRC Press, Boca Raton, FL.

Ludwig, M. L., Schopfer, L. M., Metzger, A. L., Pattridge, K. A., & Massey, V. (1990) *Biochemistry 29*, 10364−10375.

Mayhew, S. G., & Ludwig, M. L. (1975) *Enzymes (3rd Ed.) 12*, 57−118.

Moonen, C. T. W., Vervoort, J., & Müller, F. (1984) in *Flavins and Flavoproteins* (Bray, R. C., Engel, P. C., & Mayhew, S. G., Eds.) pp 493−496, de Gruyter, Berlin.

Paulsen, K. E., Stankovich, M. T., Stockman, B. J., & Markley, J. L. (1990) *Arch. Biochem. Biophys. 280*, 68−73.

Rao, S. T., Shaffie, F., Yu, C., Satyshur, K. A., Stockman, B. J., Markley, J. L., & Sundaralingam, M. (1992) *Protein Sci. 1*, 1413−1427.

Reynolds, R. A., Swenson, R. P., & Watenpaugh, K. D. (1992) *Am. Cryst. Assoc. Abstr. 20*, 130.

Simondson, R. P., & Tollin, G. (1980) *Mol. Cell. Biochem. 33*, 13−24.

Smith, W. W., Pattridge, K. A., Ludwig, M. L., Petsko, G. A., Tsernoglou, D., Tanaka, M., & Yasunobu, K. T. (1983) *J. Mol. Biol. 165*, 737−755.

Stockman, B. J., Krezel, A. M., Markley, J. L., Leonhardt, K. G., & Straus, N. A. (1990) *Biochemistry 29*, 9600−9609.

Stockman, B. J., Euvrard, A., Kloosterman, D. A., Scahill, T. A., & Swenson, R. P. (1993) *J. Biomol. NMR 3*, 133−149.

Swenson, R. P., & Krey, G. D. (1994) *Biochemistry 33*, 8505−8514.

van Mierlo, C. P. M., Lijnzaad, P., Vervoort, J., Müller, F., Berendsen, H. J. C., & de Vlieg, J. (1990) *Eur. J. Biochem. 194*, 185−198.

Watt, W., Tulinsky, A., Swenson, R. P., & Watenpaugh, K. D. (1991) *J. Mol. Biol. 218*, 195−208.

Watt, W., Reynolds, R. A., Swenson, R. P., & Watenpaugh, K. D. (1992) *Am. Cryst. Assoc. Abstr. 20*, 131.

Wüthrich, K. (1986) *NMR of Proteins and Nucleic Acids*, pp 1−292, Wiley, New York.

BI9413948